Total Effective Dose from Radiologic Emissions from INL Facilities for Calculation of Population Dose for the INL 2025 Annual Site Environmental Report

Arthur S. Rood

May 31, 2026

INTRODUCTION

Total effective radiation dose from airborne releases was calculated using air dispersion modeling utilizing the HYSPLIT model (Stein et al. 2015; Draxler et al. 2013) and performed by the National Oceanic and Atmospheric Administration (NOAA) Atmospheric Sciences Modeling Division (ASMD) on their cluster server in College Park Maryland (HYSPLIT-ASMD). The HYSPLIT-ASMD model is initialized using three-dimensional meteorological data from the Weather Research Forecasting (WRF) model utilizing high-resolution rapid response (HRRR) data assimilation. The HRRR-WRF simulation uses a 3-km grid spacing and updates the simulation every hour with surface and upper air observations. Terrain effects on winds vectors is also included in the simulation. The HYSPLIT-ASMD air dispersion results are then used in the Dose Multi-Media (DOSEMM) dose assessment model version 250619 (Rood 2019)[1]. The objective of these calculations was to provide a grid of total effective dose across a model domain that encompasses a 50-mile (80-km) radius from any Idaho National Laboratory (INL) Site source.

Population dose calculations for 2024 and prior years used a customized version of HYSPLIT run by the NOAA Special Operations and Research Division (SORD) office in Idaho Falls. This version of HYSPLIT (HYSPLIT-SORD) utilized only the surface stations from the Idaho National Laboratory (INL) meteorological monitoring network and no terrain data. A comparison of the two versions of HYSPLIT (HYSPLIT-SORD and HYSPLIT-ASMD) were reported in a technical memorandum by Arthur Rood of K-Spar Inc dated March 25th, 2026. In general, the HYSPLIT-ASMD had higher dispersion factors for most of the Site boundary receptors compared to HYSPLIT-SORD. Additionally, HYPLIT-ASMD showed significant effects of terrain such as terrain channeling and low-windspeed inversion conditions where pollutants can accumulate in low-lying areas.

Differences between the CAP88 dose estimates and those produced by HYSPLIT are documented in previous population dose reports. Most of the difference was attributed to the dispersion and deposition factors, and build-up of radionuclides in soil. The focus of this technical memorandum is to compare doses from CAP88 to HYSPLIT-ASMD/DOSEMM model at the Maximum Exposed Individual (MEI) and discuss how that has changed from previous years when HYSPLIT-SORD was used.

MODEL DOMAIN AND SOURCES

The HYSPLIT-ASMD model was used to calculate dispersion and deposition factors. Dispersion factors are defined as the monthly-average air concentration (g m^{-3}) divided by the

[1] The DOSEMM documentation (Rood 2019) is for version 190429. The difference is version 230612 has the option to use age-specific external dose coefficients from Federal Guidance Report 15 (EPA 2019) and to neglect deposition and inhalation and ingestion doses for noble gas radionuclides. These options were used for the calculations in this report; however, the receptor is an adult so results between the two versions would be identical provided the non-age-specific dose coefficients represented an adult.

release rate (g s^{-1}) and have units of s m^{-3}. Deposition factors are defined as the monthly-average deposition rate (g m^{-2} s^{-1}) divided by the release rate (g s^{-1}) and have units of m^{-2}. HYSPLIT-ASMD model results were received from Matthew Brewer of the NOAA Idaho Falls office in NetCDF format. The modeling domain parameters are presented in Table 1. The 0.02-degree grid spacing equates to approximately 2 km. The files were first processed through the utility ncdump via the Perl script *runncdumpl.pl* that produced ASCII files of the gridded concentrations and deposition data for each facility modeled.

Table 1. HYSPLIT modeling domain parameters

Parameter	Value
Model domain SW corner latitude (degrees)[a]	42.6
Model domain SW corner longitude (degrees)[a]	-114.76
Number of East-West nodes	177
Number of North-South nodes	101
Grid spacing (degrees)	0.02
Datum	WGS84
Grid center latitude (degrees)	43.6
Grid center longitude (degrees)	-113.0
Top of ground-level cell	50 m above ground level

a. These coordinates represent the SW corner of the grid cell in the SW corner of the model domain. The center of the SW cell is at 42.61 and -114.75 degrees.

Separate NetCDF files were produced for each INL Site facility (e.g., INTEC, INTEC-MS, CFA, etc.) and IRC facilities (Table 2). Within each file, concentration data for three species were provided. Average monthly ground-level concentration output (in units of g m^{-3}) was provided in the variables con1, con2, and con3. The variable con1 was for concentration of a tracer (i.e., non-decaying non-depositing) gas. The variable con2 was for the concentration of a particulate with a dry deposition velocity of 0.0018 m s^{-1}, and the variable con3 was for the concentration of a reactive gas with a deposition velocity of 0.035 m s^{-1}. Monthly deposition output (in units of g m^{-2}) was provided in the variable dep2 and dep3 corresponding to species 2 and 3. There was no deposition output for species 1 as it is a gas. All concentration and deposition values were based on a constant source release rate of 1 g s^{-1}. The model grid and species modeled were identical to those produced in prior years by HYSPLIT-SORD.

Table 2. Facilities modeled with HYSPLIT-ASMD and release parameters.

Facility	File Designation	Latitude and Longitude (degrees)	Release parameters
Advanced Test Reactor (ATR) Complex ATR stack	ATR_stack	43.589, -112.9671	Ht: 76.2 m, Stack dia: 1.524 m, Exit vel: 9.928 m/s, Temp: 293 K
ATR Complex, surface release	ATR_surface	43.5878, -112.9643	Ht: 0 m
ATR MTR stack	MTR_stack	43.58599, -112.9613	Ht: 76.2 m, Stack dia: 1.52 m, Exit vel: 2.4 m/s, Temp: 293 K
Central Facilities Area (CFA)	CFA_surface	43.529, -112.9441	Ht: 0 m
Critical Infrastructure Test Range Complex (CITRC)	CITRC_surface	43.5504, -112.8593	Ht: 0 m
Idaho Nuclear Technology and Engineering Center (INTEC), main stack[c] (MS)	INTEC_stack	43.572, -112.9336	Ht: 76.2 m, Stack dia: 1.83 m, Exit vel: 10.387 m/s, Temp: 293 K
Idaho Nuclear Technology and Engineering Center surface release	INTEC_surface	43.572, -112.9336	Ht: 0 m

Facility	File Designation	Latitude and Longitude (degrees)	Release parameters
Materials and Fuels Complex (MFC) surface release	MFC_surface	43.5951, -112.6567	Ht: 0 m
MFC, main stack	MFC_stack	43.5951, -112.6567	Ht: 60 m, Stack dia: 1.52 m, Exit vel: 8.799 m/s, Temp: 293 K
MFC, Transient Reactor Test Facility (TREAT) stack	TREAT_stack	43.60183, -112.6701	Ht: 42.7 m, Stack dia: 0.61 m, Exit vel: 5.17 m/s, Temp: 293 K
Naval Reactors Facility	NRF_surface	43.6489, -112.9162	Ht: 0 m
NETP	NETP_surface	43.7019, -112.6896	Ht: 0 m
Radioactive Waste Management Complex (RWMC)	RWMC_surface	43.4999, -113.0407	Ht: 0 m
Radioactive Release Test Range	RRTR_surface	43.8724, -112.7273	Ht: 0 m
RTP	RTP_surface	43.6690, -112.6995	Ht: 0 m
Specific Manufacturing Capability (SMC)	SMC_surface	43.8579, -112.73077	Ht: 0 m
Test Area North (TAN)	TAN_surface	43.8487, -112.7025	Ht: 0 m
Radiological and Environmental Sciences Laboratory (RESL), Buildings IF-683, IF-611, and IF-603[a]	RESL_surface	43.5159, -112.0348	Ht: 10 m, Exit Vel 0 m/s (no plume rise)

a. All three sources are located at the INL Research Center and were assumed to be released from the RESL stack location.

SOURCE TERM

The radionuclide source term for facilities that contributed significantly to the annual dose was determined using CAP88 version 4.1 (EPA 2019) modeling performed for the annual INL NESHAPs[2] report for radionuclides (INL 2026). These sources and radionuclides were included in the HYSPLIT-ASMD/DOSEMM modeling. Radionuclides that yielded a dose greater than 0.001% of the total dose at the location of the maximally exposed individual (MEI) for the INL Site were selected (Table 3, Table 4, and Table 5). The INL Site MEI for 2025 was Receptor 26 near the INL east entrance. If a source did not release a significant radionuclide, then that source was not modeled.

For the IRC sources in Idaho Falls, radionuclides that result in a dose greater than 0.1% of the total dose at the MEI location in Idaho Falls were included (Table 6). The in-town MEI receptor (Receptor 1) is located south of the IRC. Output from the CAP88 post-processing databases was used for this task.

[2] The National Emission Standards for Hazardous Air Pollutants (NESHAPs) report for radionuclides is produced annually for all U.S. Department of Energy facilities that emit any radionuclides other than radon-222 and radon-220 into the air according to 40 CFR part 61, Subpart H.

Table 3. Particulate radionuclide source term (Ci yr^{-1}) for radionuclide-facility combinations that contributed greater than 0.01% of the total dose for INL Site facilities at the MEI location.

Source	Br-82	Cl-36	Co-60	Cs-134	Cs-137	Eu-152	Ni-63
CFA	1.50E-01	2.06E-04			2.31E-10		1.20E-25
CITRC							
INTEC		3.14E-07	1.24E-02		9.62E-05	2.04E-09	1.29E+00
INTEC-MS					7.46E-05		
MFC	6.67E-09	7.20E-03		3.82E-04	8.73E-03		
MFC-MS							
MFC-TREAT							
NRF			7.72E-06		5.34E-05	2.22E-10	7.39E-06
RTC[a]			4.68E-03	3.37E-05	5.02E-03	5.84E-05	
RTC-ATR[a]					1.02E-04	1.58E-03	
RTC-MTR[a]							
RWMC							
SMC							
TAN-TSF							
Total	1.50E-01	7.40E-03	1.71E-02	4.16E-04	1.41E-02	1.64E-03	1.29E+00
Source	P-32	Pu-239	Sr-90	U-234	U-235	U-238	
CFA	9.71E-02	1.19E-10	1.75E-15	6.37E-13	2.08E-14	4.09E-14	
CITRC							
INTEC		4.97E-06	7.07E-05	3.47E-07	1.96E-08	1.44E-07	
INTEC-MS		3.80E-08	6.64E-05				
MFC	1.17E-05	2.41E-07	2.12E-03	7.98E-02	3.85E-03	1.22E-01	
MFC-MS		2.78E-08	6.60E-07				
MFC-TREAT		8.89E-09	1.34E-07				
NRF		1.72E-06	3.73E-05				
RTC[a]		8.44E-06	2.98E-02				
RTC-ATR[a]			3.00E-08				
RTC-MTR[a]							
RWMC		2.45E-06	8.04E-11		8.19E-13	3.38E-11	
SMC				1.08E-08	3.59E-10	3.00E-08	
TAN-TSF			3.01E-05				
Total	9.71E-02	1.79E-05	3.21E-02	7.98E-02	3.85E-03	1.22E-01	

a. The Advanced Test Reactor (ATR) Complex was formerly known as the Test Reactor Area (TRA) and Reactor Technology Complex (RTC). Acronyms based on former names may still be used to describe facility buildings, meteorological stations, etc.

Table 4. Noble gases source term (Ci yr^{-1}) for radionuclide-facility combinations that contributed greater than 0.01% of the total dose for INL Site facilities at the MEI location.

Source	Ar-41	Kr-85m	Kr-87	Kr-88	Kr-89	Xe-135	Xe-138
CFA	1.69E-14	6.03E-05	1.12E-06	7.69E-05		9.53E-02	
CITRC							
INTEC							
INTEC-MS							
MFC							
MFC-MS							
MFC-TREAT	7.28E+01	8.99E+00	9.42E+00	8.56E+00	3.08E+01	2.35E+00	1.46E+01
NRF							
RTC[a]	3.46E-02	4.65E-06	1.66E-05	1.31E-05		1.02E-03	5.95E-05
RTC-ATR[a]	1.36E+03		9.34E-02			2.66E+01	2.12E+00
RTC-MTR[a]							
RWMC							
SMC							
TAN-TSF							
Total	1.43E+03	8.99E+00	9.51E+00	8.56E+00	3.08E+01	2.91E+01	1.67E+01

a. The Advanced Test Reactor (ATR) Complex was formerly known as the Test Reactor Area (TRA) and Reactor Technology Complex (RTC). Acronyms based on former names may still be used to describe facility buildings, meteorological stations, etc

Table 5. Iodine, C-14, and H-3 source term (Ci yr^{-1}) for radionuclide-facility combinations that contributed greater than 0.01% of the total dose for INL Site facilities at the MEI location.

Source	H-3	C-14
CFA	3.30E-01	
CITRC	2.09E-04	
INTEC	2.26E-01	1.29E+00
INTEC-MS	1.28E-03	
MFC	2.45E+00	
MFC-MS		
MFC-TREAT		
NRF	4.40E-02	5.00E-01
RTC[a]	2.31E+00	
RTC-ATR[a]	8.73E+01	
RTC-MTR[a]	2.80E+00	
RWMC	1.24E+02	3.66E-02
SMC		
TAN-TSF	1.45E-02	
Total	2.19E+02	1.83E+00

a. The Advanced Test Reactor (ATR) Complex was formerly known as the Test Reactor Area (TRA) and Reactor Technology Complex (RTC). Acronyms based on former names may still be used to describe facility buildings, meteorological stations, etc.

Table 6. Radionuclide source term (Ci yr^{-1}) for radionuclides that contributed greater than 0.1% of the total dose for INL facilities in Idaho Falls.

Radionuclide	IF-603	IF-683 (RESL)	Total
Ac-227		4.75E-09	4.75E-09
Am-241	8.35E-14	1.02E-07	1.02E-07
Am-243		2.09E-09	2.09E-09
Ba-133		2.76E-07	2.76E-07
Cl-36		1.15E-08	1.15E-08
Co-60		2.22E-08	2.22E-08
Cs-134		2.87E-08	2.87E-08
Cs-137	9.11E-11	6.55E-08	6.56E-08
Eu-152	2.08E-14	3.64E-08	3.64E-08
Eu-154		1.36E-07	1.36E-07
H-3		1.20E-04	1.20E-04
I-125		1.03E-07	1.03E-07
Na-22		4.11E-08	4.11E-08
Np-237		6.48E-09	6.48E-09
Pa-231	1.39E-17	1.15E-09	1.15E-09
Pb-210		4.42E-08	4.42E-08
Pu-238		7.59E-08	7.59E-08
Pu-239	4.21E-13	1.32E-07	1.32E-07
Ra-226	5.92E-17	7.51E-08	7.51E-08
Sr-90		6.40E-08	6.40E-08
U-232		3.06E-08	3.06E-08
U-233		1.64E-07	1.64E-07
Xe-133	5.40E-01		5.40E-01

DOSEMM MODELING AND RESULTS

The DOSEMM model version 250619 (Rood 2019) was used to calculate total effective dose across the model domain for a fixed receptor scenario. DOSEMM reads the dispersion and deposition factors produced by HYSPLIT-ASMD and the source term summarized in Table 3, Table 4, Table 5, and Table 6. The dispersion and deposition factors and source term are used in combination with a food-chain and exposure model in DOSEMM to calculate radionuclide concentrations in air, soil, vegetables, meat, and milk, and calculate the associated doses from inhalation, ingestion, and external exposure.

The DOSEMM modeling used the same parameters and protocol used in previous population dose assessments and is not repeated here. The focus instead is on 1) the location of the MEI using HYSPLIT-ASMD, 2) the X/Q at the MEI for CAP88 and HYSPLIT-ASMD, and 3) the total dose at the MEI from CAP88 and HYSPLIT-ASMD/DOSEMM.

Note on Dose Coefficients

Population dose calculations in ASERs prior to 2023 were calculated with dose coefficients from DOE-Std-1196-2011 (DOE 2011) and FGR-13 (EPA 1999). For ASER population dose calculations from 2023 onwards, the most up-to-date dose coefficients were used as represented by

DOE-Std-1196-2022 (DOE 2022) and Federal Guidance Report 15 (EPA 2019). CAP88 uses dose coefficients from DOE-Std-1196-2011.

INL Site MEI Doses

The HYSPLIT-ASMD/DOSEMM model was used to compute the effective dose at all 31 Site boundary receptors. Since 2019, the MEI has been at the receptor 26 location (see Figure 1) south-southeast of the MFC facility (-112.602013 longitude, 43.526498 latitude, UTM Zone 12 370542E 4820531N).

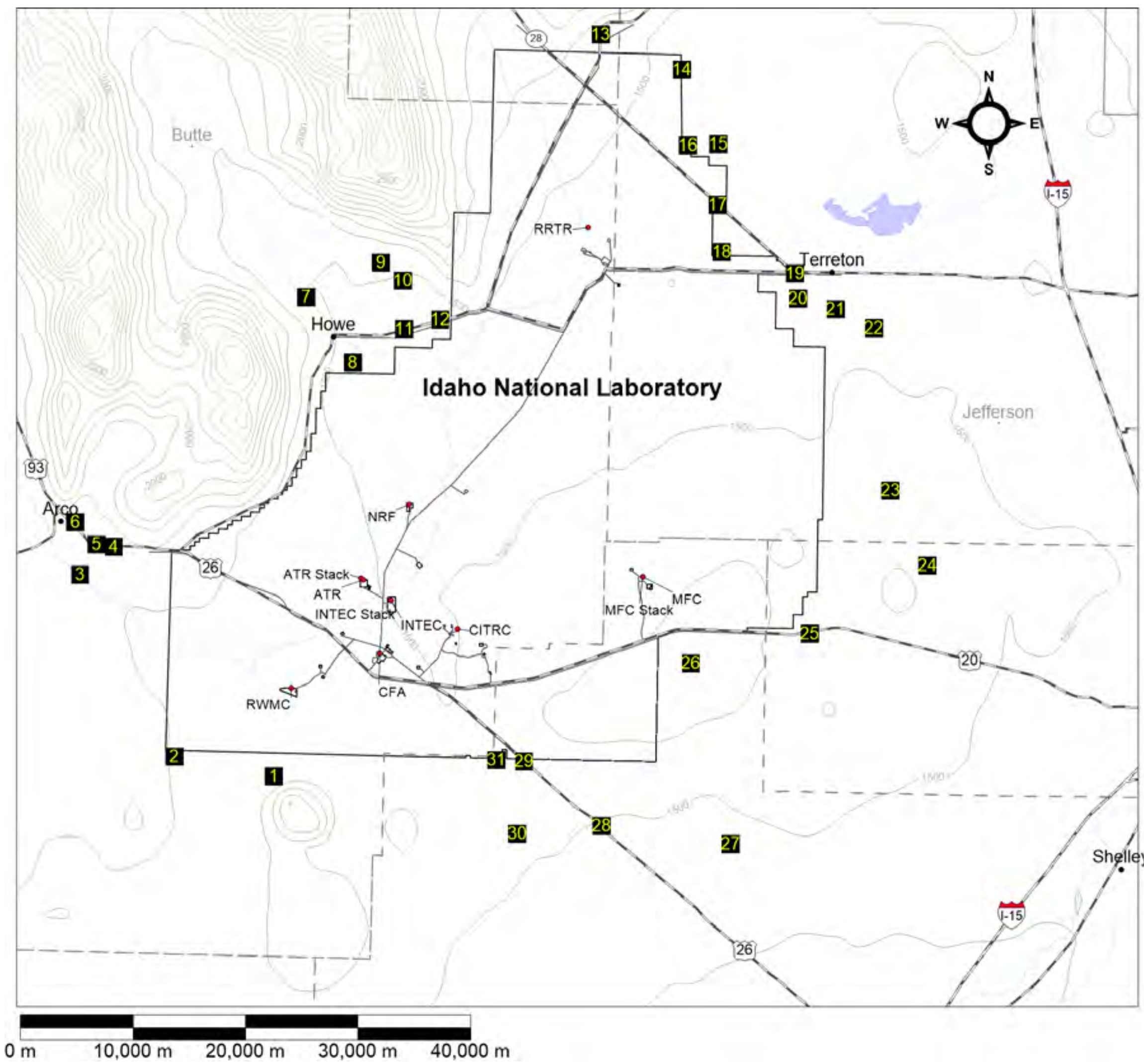

Figure 1. Site boundary receptor locations surrounding the INL Site. The 31 locations (black squares) are used in the CAP88 modeling and are from Overin et al., (2023).

The HYSPLIT-ASMD/DOSEMM-calculated doses at all 31 Site boundary receptors (Table 7) shows that the MEI location differs from that identified by CAP88. Instead of receptor 26, the MEI calculated by HYSPLIT-ASMD DOSEMM was receptor 31, which lies about 20 km WSW of receptor 26. Important radionuclides at the HYSPLIT-ASMD DOSEMM MEI receptor (receptor 31) are shown in Table 7. Population doses for previous years that used HYSPLIT-SORD had the same MEI as CAP88 at receptor 26.

The discrepancy between the MEI location defined by HYSPLIT-ASMD DOSEMM and CAP88 is thought to be attributed to inclusion of terrain in the HYSPLIT-ASMD runs. Figure 2 shows the average U-238 air concentration from MFC surface releases, which accounts for most of the dose at the MEI. Receptor 26 lies in an elevated region (~1640 m) above MFC (el ~1572 m). The HYSPLIT-ASMD simulation appears to channel the plume to the west away from elevated region around receptor 26 and funnel it to receptor 31 which lies at a lower elevation (~1526 m). This type of behavior would be expected when winds out of the north-northeast occur during stable atmospheric conditions and valley inversions.

Dispersion factors from HYSPLIT-ASMD at receptor 26 and 31 for MFC releases were 5.78E-9 s/m^3 and 5.51E-08 s/m^3 respectively. Thus, concentrations at receptor 31 are about an order of magnitude higher than receptor 26.

Table 7. HYSPLIT-ASMD/DOSEMM annual effective doses for 2025 at the 31 Site boundary receptors (mrem/y). The MEI was receptor 31 having a total dose of 2.51E-02 mrem/y.

Receptor	Br-82	Cl-36	Co-60	Cs-134	Cs-137	Eu-152	Ni-63	P-32
1	7.16E-06	1.86E-04	6.30E-05	4.55E-07	3.48E-05	9.48E-07	1.50E-05	1.26E-05
2	4.74E-07	4.26E-05	1.37E-05	1.33E-07	1.08E-05	1.02E-06	2.63E-06	1.21E-06
3	4.87E-07	8.12E-05	1.21E-05	1.92E-07	1.03E-05	1.01E-06	2.67E-06	1.29E-06
4	9.22E-07	1.59E-04	2.09E-05	3.68E-07	1.85E-05	1.62E-06	4.77E-06	2.33E-06
5	1.02E-06	1.94E-04	2.36E-05	4.44E-07	2.15E-05	1.91E-06	5.41E-06	2.59E-06
6	4.88E-07	9.60E-05	1.22E-05	2.20E-07	1.08E-05	1.01E-06	2.80E-06	1.31E-06
7	3.12E-06	1.01E-04	3.27E-05	2.96E-07	2.28E-05	1.37E-06	7.15E-06	3.81E-06
8	2.32E-06	1.44E-04	6.30E-05	5.03E-07	4.52E-05	1.84E-06	1.30E-05	4.94E-06
9	2.53E-06	2.06E-04	4.38E-05	5.41E-07	3.45E-05	1.91E-06	9.48E-06	4.34E-06
10	4.23E-06	4.59E-04	9.28E-05	1.19E-06	7.26E-05	3.64E-06	2.06E-05	8.71E-06
11	4.53E-06	2.57E-04	9.14E-05	8.02E-07	6.43E-05	2.50E-06	1.98E-05	7.83E-06
12	5.36E-06	2.51E-04	9.77E-05	7.83E-07	6.46E-05	2.82E-06	2.19E-05	8.98E-06
13	6.13E-07	7.34E-05	6.63E-06	1.60E-07	6.62E-06	3.95E-07	1.55E-06	8.32E-07
14	1.08E-06	1.32E-04	1.04E-05	2.85E-07	1.11E-05	5.76E-07	2.38E-06	1.30E-06
15	1.67E-06	2.60E-04	1.51E-05	5.47E-07	1.90E-05	7.80E-07	3.45E-06	1.88E-06
16	1.59E-06	2.29E-04	1.46E-05	4.86E-07	1.75E-05	7.82E-07	3.32E-06	1.79E-06
17	2.05E-06	3.84E-04	2.04E-05	7.99E-07	2.65E-05	1.02E-06	4.84E-06	2.55E-06
18	2.32E-06	6.74E-04	2.49E-05	1.38E-06	4.09E-05	1.20E-06	6.05E-06	3.20E-06
19	2.18E-06	1.37E-03	2.21E-05	2.73E-06	6.95E-05	1.01E-06	5.52E-06	3.10E-06
20	2.38E-06	1.81E-03	2.31E-05	3.58E-06	8.90E-05	1.00E-06	5.84E-06	3.46E-06
21	2.16E-06	1.73E-03	1.99E-05	3.42E-06	8.42E-05	8.81E-07	5.02E-06	3.10E-06
22	1.85E-06	1.55E-03	1.48E-05	3.05E-06	7.41E-05	6.71E-07	3.77E-06	2.57E-06
23	1.16E-06	1.26E-03	7.12E-06	2.42E-06	5.77E-05	3.24E-07	1.85E-06	1.62E-06
24	5.58E-07	4.71E-04	4.39E-06	9.08E-07	2.24E-05	1.98E-07	1.13E-06	9.29E-07

25	7.38E-07	5.65E-04	5.80E-06	1.09E-06	2.70E-05	2.55E-07	1.50E-06	1.33E-06
26	3.90E-07	7.61E-04	2.89E-06	1.45E-06	3.43E-05	1.20E-07	7.34E-07	6.91E-07
27	5.88E-07	8.94E-04	9.02E-06	1.73E-06	4.28E-05	4.03E-07	2.38E-06	1.92E-06
28	1.01E-06	1.68E-03	9.89E-06	3.24E-06	7.74E-05	4.07E-07	2.61E-06	2.47E-06
29	2.98E-06	3.99E-03	2.44E-05	7.69E-06	1.83E-04	3.13E-07	6.43E-06	7.88E-06
30	3.07E-06	2.08E-03	1.80E-05	4.01E-06	9.69E-05	2.83E-07	4.90E-06	6.91E-06
31	6.47E-06	4.73E-03	3.76E-05	9.12E-06	2.18E-04	3.86E-07	1.03E-05	1.48E-05

Receptor	Pu-239	Sr-90	U-234	U-235	U-238	Ar-41	Kr-85m	Kr-87
1	4.10E-06	2.38E-04	1.75E-04	8.99E-06	2.67E-04	5.78E-04	1.88E-07	4.74E-07
2	9.26E-07	7.51E-05	4.88E-05	2.50E-06	7.43E-05	4.75E-04	4.68E-08	1.05E-07
3	8.68E-07	5.74E-05	1.13E-04	5.80E-06	1.72E-04	6.77E-04	1.57E-07	2.74E-07
4	1.70E-06	9.91E-05	2.44E-04	1.25E-05	3.71E-04	1.53E-03	4.09E-07	7.75E-07
5	1.90E-06	1.11E-04	3.04E-04	1.55E-05	4.60E-04	1.75E-03	4.71E-07	8.49E-07
6	9.50E-07	5.63E-05	1.45E-04	7.42E-06	2.20E-04	8.48E-04	2.20E-07	3.72E-07
7	2.49E-06	1.56E-04	1.33E-04	6.82E-06	2.03E-04	9.74E-04	2.02E-07	5.06E-07
8	4.82E-06	3.28E-04	1.72E-04	8.82E-06	2.62E-04	1.39E-03	2.25E-07	7.18E-07
9	3.35E-06	2.17E-04	3.04E-04	1.55E-05	4.61E-04	1.44E-03	4.79E-07	1.27E-06
10	7.41E-06	4.48E-04	6.90E-04	3.53E-05	1.05E-03	2.99E-03	1.12E-06	3.21E-06
11	7.28E-06	4.48E-04	3.42E-04	1.75E-05	5.20E-04	1.74E-03	4.66E-07	1.51E-06
12	7.61E-06	4.52E-04	3.27E-04	1.67E-05	4.97E-04	1.91E-03	4.74E-07	1.61E-06
13	4.84E-07	2.99E-05	1.08E-04	5.50E-06	1.63E-04	1.10E-04	1.16E-07	1.96E-07
14	7.05E-07	4.76E-05	1.76E-04	9.02E-06	2.68E-04	1.52E-04	2.03E-07	3.79E-07
15	9.66E-07	7.03E-05	3.43E-04	1.76E-05	5.22E-04	2.17E-04	4.01E-07	9.15E-07
16	9.46E-07	6.84E-05	3.04E-04	1.55E-05	4.62E-04	2.20E-04	3.51E-07	8.16E-07
17	1.25E-06	9.01E-05	5.09E-04	2.61E-05	7.75E-04	3.04E-04	6.00E-07	1.64E-06
18	1.53E-06	1.11E-04	9.41E-04	4.82E-05	1.43E-03	4.23E-04	1.09E-06	3.38E-06
19	1.34E-06	1.10E-04	2.01E-03	1.03E-04	3.05E-03	3.67E-04	1.89E-06	5.72E-06
20	1.43E-06	1.22E-04	2.70E-03	1.38E-04	4.10E-03	4.13E-04	2.50E-06	8.07E-06
21	1.25E-06	1.09E-04	2.59E-03	1.32E-04	3.93E-03	3.52E-04	2.35E-06	7.28E-06
22	9.48E-07	8.63E-05	2.33E-03	1.19E-04	3.54E-03	2.73E-04	2.11E-06	6.34E-06
23	4.96E-07	5.18E-05	1.91E-03	9.78E-05	2.90E-03	1.64E-04	1.45E-06	5.37E-06
24	2.84E-07	2.54E-05	6.87E-04	3.52E-05	1.04E-03	7.31E-05	5.25E-07	1.80E-06
25	3.92E-07	3.23E-05	8.51E-04	4.35E-05	1.29E-03	1.28E-04	7.49E-07	3.54E-06
26	1.96E-07	2.68E-05	8.47E-04	4.35E-05	1.29E-03	8.24E-05	4.22E-07	2.52E-06
27	7.45E-07	5.11E-05	1.48E-03	7.56E-05	2.24E-03	2.79E-04	2.21E-06	7.63E-06
28	8.60E-07	7.11E-05	2.76E-03	1.41E-04	4.18E-03	4.25E-04	3.69E-06	1.41E-05
29	1.69E-06	1.67E-04	6.30E-03	3.22E-04	9.56E-03	5.90E-04	6.28E-06	2.70E-05
30	1.46E-06	1.01E-04	3.26E-03	1.67E-04	4.94E-03	3.43E-04	3.34E-06	1.17E-05
31	2.58E-06	2.11E-04	7.25E-03	3.71E-04	1.10E-02	6.85E-04	7.13E-06	2.95E-05

Receptor	Kr-88	Kr-89	Xe-135	Xe-138	C-14	H-3	Total	
1	3.43E-06	2.11E-23	3.54E-06	3.68E-08	1.33E-04	4.58E-04	2.18E-03	
2	8.08E-07	1.60E-27	3.12E-06	1.26E-08	2.79E-05	8.28E-05	8.61E-04	
3	2.61E-06	1.89E-29	4.76E-06	1.09E-08	4.74E-05	8.89E-05	1.28E-03	
4	6.95E-06	1.42E-27	1.00E-05	4.60E-08	1.10E-04	1.87E-04	2.77E-03	
5	7.91E-06	2.85E-28	1.19E-05	3.73E-08	1.24E-04	2.13E-04	3.24E-03	
6	3.63E-06	1.41E-29	6.12E-06	1.11E-08	5.62E-05	1.14E-04	1.58E-03	
7	3.66E-06	9.45E-24	6.93E-06	1.47E-08	1.40E-04	1.72E-04	1.96E-03	
8	4.31E-06	2.43E-20	8.37E-06	8.56E-08	2.44E-04	2.23E-04	2.91E-03	
9	8.86E-06	3.68E-22	1.10E-05	1.60E-08	2.06E-04	2.37E-04	3.20E-03	
10	2.12E-05	1.39E-20	2.21E-05	5.22E-08	5.00E-04	4.89E-04	6.89E-03	
11	9.01E-06	2.57E-19	1.15E-05	6.72E-08	4.16E-04	3.01E-04	4.25E-03	
12	9.27E-06	1.30E-18	1.31E-05	6.52E-08	4.50E-04	3.27E-04	4.45E-03	
13	1.95E-06	6.08E-29	1.62E-06	5.99E-11	2.46E-05	3.73E-05	5.71E-04	
14	3.49E-06	3.13E-27	2.25E-06	2.08E-10	3.71E-05	5.13E-05	9.04E-04	
15	7.22E-06	5.87E-24	2.94E-06	1.77E-09	4.77E-05	6.44E-05	1.59E-03	
16	6.34E-06	9.75E-24	2.85E-06	1.78E-09	4.80E-05	6.31E-05	1.46E-03	
17	1.13E-05	3.55E-21	3.70E-06	9.56E-09	6.09E-05	7.87E-05	2.30E-03	
18	2.10E-05	5.77E-19	4.80E-06	4.53E-08	7.52E-05	9.75E-05	3.90E-03	
19	3.63E-05	4.40E-19	4.58E-06	6.59E-08	6.64E-05	9.08E-05	7.32E-03	
20	4.88E-05	4.51E-18	5.01E-06	1.35E-07	6.97E-05	9.74E-05	9.63E-03	
21	4.54E-05	1.16E-18	4.49E-06	9.62E-08	5.89E-05	9.01E-05	9.17E-03	
22	4.06E-05	3.37E-19	3.64E-06	6.80E-08	4.27E-05	7.17E-05	8.17E-03	
23	2.92E-05	2.81E-16	1.93E-06	2.14E-07	1.90E-05	4.07E-05	6.55E-03	
24	1.04E-05	7.67E-18	9.34E-07	4.45E-08	1.12E-05	2.38E-05	2.41E-03	
25	1.60E-05	4.68E-13	1.27E-06	6.26E-07	1.55E-05	3.48E-05	3.02E-03	
26	9.48E-06	6.55E-10	6.43E-07	1.89E-06	7.48E-06	1.69E-05	3.13E-03	
27	4.37E-05	4.09E-17	3.05E-06	1.97E-07	3.36E-05	7.65E-05	5.25E-03	
28	7.48E-05	2.11E-15	3.99E-06	6.88E-07	3.56E-05	9.32E-05	9.58E-03	
29	1.31E-04	1.78E-13	5.11E-06	2.71E-06	6.74E-05	1.62E-04	2.16E-02	
30	6.63E-05	9.92E-17	3.28E-06	3.31E-07	6.20E-05	1.76E-04	1.13E-02	
31	1.47E-04	5.25E-14	5.96E-06	2.31E-06	1.10E-04	2.76E-04	**2.51E-02**	MEI

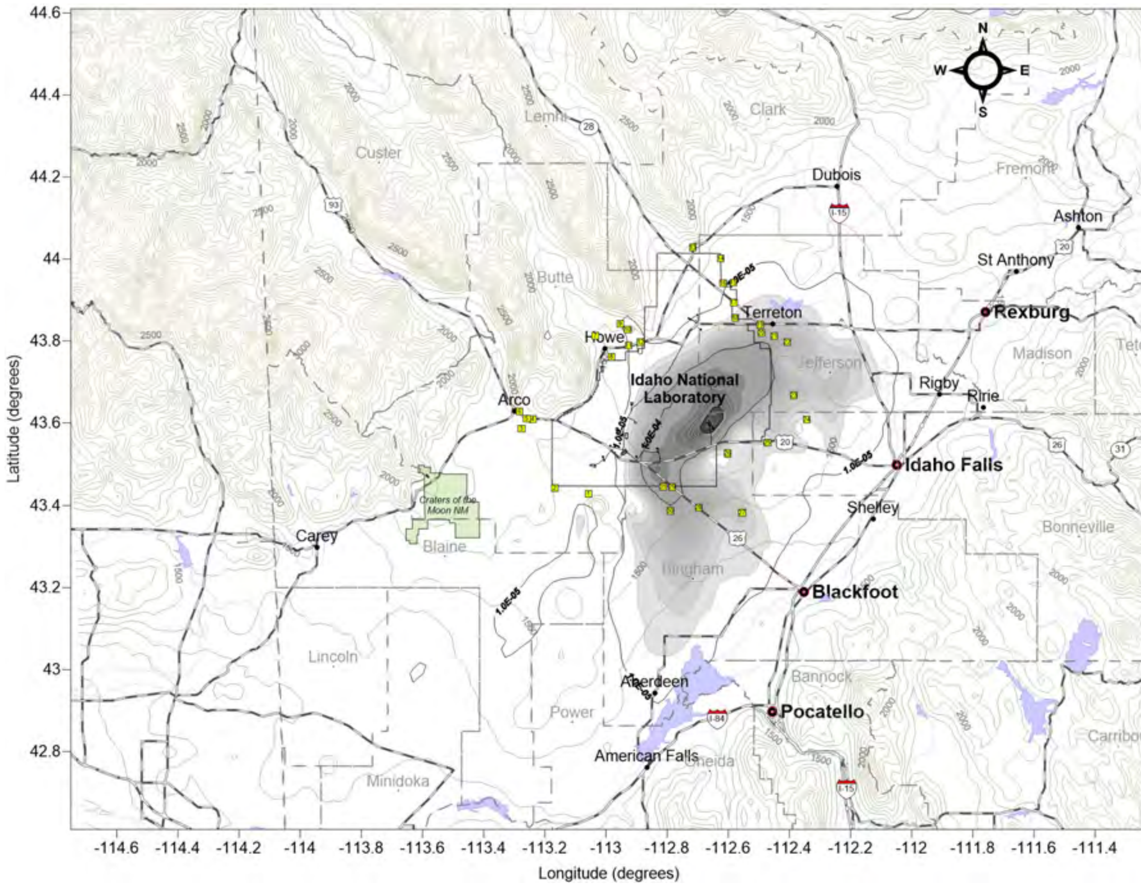

Figure 2. Isopleth map of average U-238 concentration (pCi/m^3) from MFC surface releases for 2025 using the HYSPLIT-ASMD/DOSEMM models. Note that the plume flows around receptor 26 (south of MFC) which is located in an elevated region.

Annual effective dose by radionuclide at the MEI receptor (31) (Table 8) shows that U-238, U-234, and Cl-36 are the primary dose contributors accounting for over 90% of the total dose. This order agrees with CAP88 annual effective dose at receptor 26 but these radionuclides only account for 83% of the total in CAP88. The total CAP88 annual effective dose at the MEI (receptor 26) was 0.0245 mrem/y and was slightly less than HYSPLIT-ASMD/DOSEMM annual effective dose of 0.0251 mrem/y at receptor 31. The CAP88 X/Q at receptor 26 was 3.94E-08 s/m^3 which was slightly less than the HYSPLIT-ASMD/DOSEMM X/Q of 5.51E-08 s/m^3 at receptor 31.

Another important radionuclide is Ar-41 released from both MFC-TREAT and RTC-ATR. CAP88 X/Qs at the MEI (receptor 26) were 5.14E-10 s/m^3 for RTC-ATR and 1.64E-08 s/m^3 for MFC-TREAT. The corresponding X/Q values at the HYSPLIT-ASMD/DOSEMM MEI (receptor 31) were 1.18E-09 s/m^3 for RTC-ATR and 4.37E-08 s/m^3 for MFC-TREAT. Consequently, Ar-41 is the 4th highest dose contributor at the MEI for HYSPLIT-ASMD/DOSEMM whereas Ar-41 is the 7th highest dose contributor for CAP88. Thus, some of the difference between CAP88 and HYSPLIT-ASMD/DOSEMM doses are attributed to differences in the X/Q values. CAP88 generally has higher doses for food ingestion and external exposure because radionuclides are allowed to build up in soil over a 100-year period whereas in DOSEMM build-up is only for a year.

Table 8. Annual effective doses by radionuclide at the MEI receptor (31) for the HYSPLIT-ASMD/DOSEMM model.

Radionuclide	Doses (mrem)	Percent of Total	Cumulative
U-238	1.10E-02	43.81%	43.81%
U-234	7.25E-03	28.85%	72.66%
Cl-36	4.73E-03	18.81%	91.47%
Ar-41	6.85E-04	2.72%	94.19%
U-235	3.71E-04	1.48%	95.67%
H-3	2.76E-04	1.10%	96.77%
Cs-137	2.18E-04	0.87%	97.63%
Sr-90	2.11E-04	0.84%	98.47%
Kr-88	1.47E-04	0.59%	99.06%
C-14	1.10E-04	0.44%	99.50%
Co-60	3.76E-05	0.15%	99.65%
Kr-87	2.95E-05	0.12%	99.76%
P-32	1.48E-05	0.06%	99.82%
Ni-63	1.03E-05	0.04%	99.86%
Cs-134	9.12E-06	0.04%	99.90%
Kr-85m	7.13E-06	0.03%	99.93%
Br-82	6.47E-06	0.03%	99.96%
Xe-135	5.96E-06	0.02%	99.98%
Pu-239	2.58E-06	0.01%	99.99%
Xe-138	2.31E-06	0.01%	100.00%
Eu-152	3.86E-07	0.00%	100.00%
Kr-89	5.25E-14	0.00%	100.00%
Total (mrem)	**2.51E-02**	**100.00%**	

INL In-Town MEI Doses

The highest dose from INL in-town sources (includes the Idaho Research Center [IRC] and RESL) was calculated at the nearest HYSPLIT-ASMD model node northeast of the IRC (1,139 m, azimuth bearing 2.07 degrees) of the RESL/IRC facility (longitude -112.03412, latitude 43.51462 HYSPLIT-ASMD node number 8279). This location represents the HYSPLIT-ASMD node nearest to the intown receptor number 19 (952 m azimuth 4.03 degrees from building IF-603). The HYSPLIT grid resolution (about 2 km) was such that close in receptors could not be represented. All 30 of the potential MEI in-town receptors were run and DOSEMM assigns the closest grid node to each receptor. This location was the same as the MEI location calculated with HYSPLIT-SORD and the X/Qs were similar; 1.61E-6 s/m^3 for HYSPLIT-ASMD for 2025 and 1.42E-06 s/m^3 for HYSPLIT-SORD for 2023. The CAP88 MEI for IRC sources was 147m south of the IRC. Consequently, CAP88 MEI doses for IRC sources were substantially higher (4.5E-03 mrem/y) than those from HYSPLIT-ASMD/DOSEMM (4.52E-05 mrem/y).

TOTAL EFFECTIVE DOSE ISOPLETH MAP

An isopleth map of total effective dose across the model domain based on the MEI receptor scenario is shown in Figure 3. The INL Site MEI location (receptor 31) is located at the intersection of the southern INL Site boundary and US Highway 26. The isopleths reflect the southwest to northeast prevailing winds at the INL and terrain features, which for the HYSPLIT-ASMD model are explicitly modeled and make a significant difference in the plume pattern. For example, there are plume lobes going up the valleys northwest of Arco and Howe. The isopleth map for the 2023 ASER (Figure 4) was performed using HYSPLIT-SORD model and exhibits a more compact plume and little terrain influence other than what would be inferred from the surface meteorological stations. The overall extent of the plume is larger using HYSPLIT-ASMD and therefore, population doses would be expected to be higher than those that would be calculated using HYSPLIT-SORD.

An ASCII text file containing the effective dose by exposure pathway at each of the model grid nodes is provided in the file *EffectiveTotal.dat*. As expected, doses from the Idaho Falls facilities were not discernable in the dose contours.

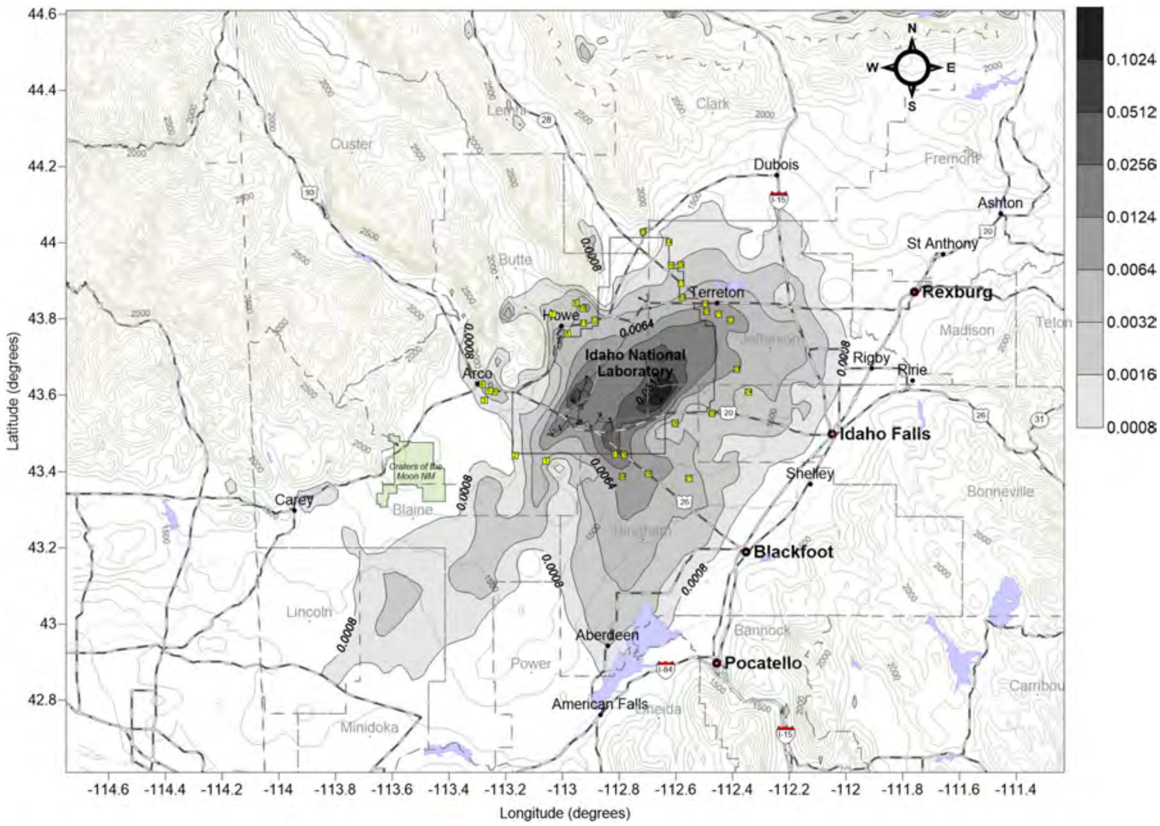

Figure 3. Isopleth map to total effective dose (mrem/y) for 2025 releases based on the MEI exposure scenario and the HYSPLIT-ASMD/DOSEMM model. The INL Site MEI based on this model was receptor 31 located at the intersection of the southern INL Site boundary and US Highway 26.

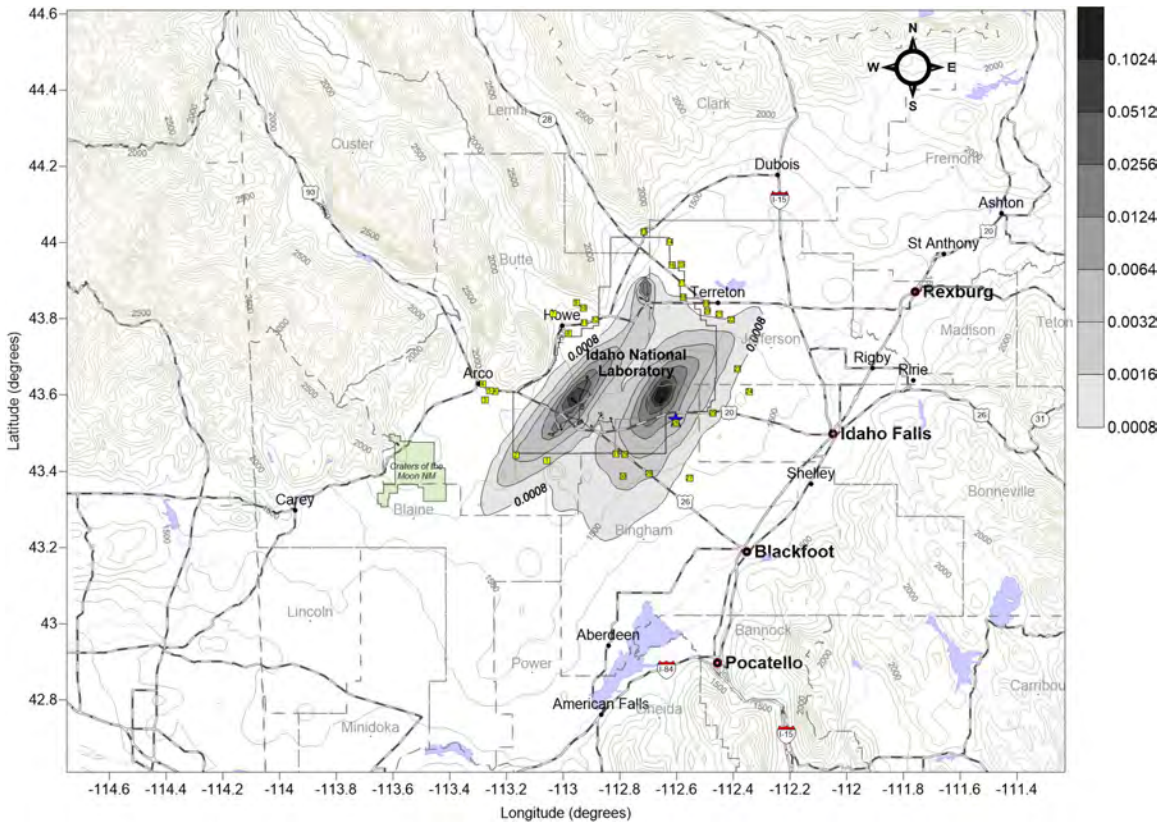

Figure 4. Isopleth map to total effective dose (mrem/y) for 2023 releases based on the MEI exposure scenario and the HYSPLIT-SORD/DOSEMM model. The INL Site MEI based on this model was receptor 26 located on the southern INL Site boundary south of MFC. The receptor is indicated by a blue star.

REFERENCES

DOE (U.S. Department of Energy), 2011. *Derived Concentration Technical Standard.* DOE-STD-1196-2011, U.S. Department of Energy, Washington DC.

DOE, 2022. *Derived Concentration Technical Standard.* DOE-STD-1196-2022, U.S. Department of Energy, Washington DC.

DOE-ID 1994. *Track 2 Sites: Guidance for Assessing Low Probability Hazard Sites at the INEL*. DOE/ID-10389, Rev 6. U.S. Department of Energy, Idaho Operations Office, January 1994.

Draxler, R.R., B. Stunder, G. Rolph, A. Stein, and A. Taylor, 2013, *HYSPLIT4 User's Guide, Version 4 revision April 2013*, http://ready.arl.noaa.gov/HYSPLIT.php, National Oceanic and Atmospheric Administration, College Park, Maryland.

EPA (U.S. Environmental Protection Agency), 1999. *Federal Guidance Report 13: Cancer Risk Coefficients for Environmental Exposure to Radionuclides*. EPA 402-R-99-001. US EPA, Washington DC.

EPA 2019, *CAP88-PC Version 4.1 User's Guide*. Trinity Engineering Associates, Inc., Cincinnati, OH, submitted to U.S. EPA, Office of Radiation and Indoor Air, Washington DC, May 2013.

EPA 2019. *Federal Guidance Report 15: External Exposure to Radionuclides in Air, Water, and Soil*. EPA 402/R19/002. US EPA, Washington DC.

Moore, R.E., C.F. Baes III, L.M. McDowell-Boyer, A.P. Watson, F.O. Hoffman, J.C. Pleasant, and C.W. Miller, 1979. AIRDOS-EPA: A Computerized Methodology for Estimating Environmental Concentrations and Dose to Man from Airborne Releases of Radionuclides. EPA 520/1-79-009. EPA Office of Radiation Programs, Washington D.C.

Overin, K.B., A.J. Sondrup, and J.P. Shive, 2023. *Update of Receptor Locations for INL National Emission Standards for Hazardous Air Pollutants*. INL/RPT-23-72759. Idaho National laboratory, Idaho Falls ID, June.

Rood, A.S., 2019. DOSEMM: A Model for Assessment of Airborne Releases and Multimedia Terrestrial Transport and Dose Assessment v190429. 01-2017-Final, Revised May, 2019. Risk Assessment Corporation, Neeses SC.

Stein, A.F., R.R. Draxler, G.D. Rolph, B.J.B. Stunder, M.D. Cohen, and F. Ngan, 2015. "NOAA's HYSPLIT atmospheric transport and dispersion modeling system", *Bull. Amer. Meteor. Soc.*, 96, 2059-2077, http://dx.doi.org/10.1175/BAMS-D-14-00110.1